Role of ceramide 1 in the molecular organization of the stratum corneum lipids

J. A. Bouwstra,[1,*] G. S. Gooris,[*] F. E. R. Dubbelaar,[*] A. M. Weerheim,[†] A. P. IJzerman[*] and M. Ponec[†]

Leiden/Amsterdam Center for Drug Research,* Gorlaeus Laboratories, Leiden University, P.O. Box 9502, 2300 RA Leiden, The Netherlands, and Department of Dermatology,† University Hospital, Leiden, The Netherlands

Abstract The main barrier of the skin is formed by the lipids in the apical skin layer, the stratum corneum (SC). In SC mainly ceramides (CER), free fatty acids (FFA) and cholesterol (CHOL) are present. The CER are composed of at least six different fractions. CER 1 has an exceptional molecular structure as it contains a linoleic acid linked to a long-chain ω-hydroxy acid (C > 30). The SC lipids are organized in two lamellar phases with periodicities of approximately 6 and 13 nm, respectively. Recent studies revealed that ceramides isolated from pig SC mixed with cholesterol in confined ratios mimic stratum corneum lipid phase behavior closely (Bouwstra, J.A., et al. 1996. *J. Lipid Res.* 37: 999–1011). In this paper the role of CER 1 for the SC lipid lamellar organization was studied. For this purpose lipid phase behavior of mixtures of CHOL and total ceramide fraction was compared with that of mixtures of CHOL and a ceramide mixture lacking CER 1. These studies showed that in the absence of CER 1 almost no long periodicity phase was formed over a wide CHOL/CER molar ratio. A model is proposed for the molecular arrangement of the two lamellar phases. This model is based on the dominant role CER 1 plays in the formation of the long periodicity phase, electron density distribution calculations, and observations, such as *i*) the bimodal distribution of the fatty acid chain lengths of the ceramides, *ii*) the phase separation between long-chain ceramides and short-chain ceramides in a monolayer approach, and *iii*) the absence of swelling of the lamellae upon increasing the water content organization in SC. In this molecular model the short periodicity phase is composed of only two high electron density regions indicating the presence of only one bilayer, similar to that often found in phospholipid membranes. The molecular arrangement in the long periodicity phase is very exceptional. This phase most probably consists of two broad and one narrow low electron density regions. The two broad regions are formed by partly interdigitating ceramides with long-chain fatty acids of approximately 24–26 C atoms, while the narrow low-electron density region is formed by fully interdigitating ceramides with a short free fatty acid chain of approximately 16 to 18 C atoms.—**Bouwstra, J. A., G. S. Gooris, F. E. R. Dubbelaar, A. M. Weerheim, A. P. IJzerman, and M. Ponec.** Role of ceramide 1 in the molecular organization of the stratum corneum lipids. *J. Lipid Res.* 1998. **39:** 186–196.

Supplementary key words stratum corneum • ceramides • phase behavior • X-ray diffraction

The main problem in dermal and transdermal drug delivery is the low penetration of drugs through the stratum corneum (SC) which is located in the uppermost layer of the skin (1). The SC consists of dead cells embedded in a lipid-rich environment. Visualization studies revealed that penetration through the SC occurs mainly intercellularly (2) indicating that the main barrier for diffusion of substances, including water and drugs, is confined to the SC intercellular lipid domains. The lipid organization in the SC has been studied by several methods, such as electron microscopy (3–5), X-ray diffraction and Fourier transform infrared spectroscopy (6, 7). These studies revealed that the lipids are organized in lamellae oriented approximately parallel to the corneocyte surface. Two lamellar phases could be identified with repeat distances of approximately 6 and 13 nm (6–9). The lateral packing of the lipids is mainly crystalline and hexagonal (8–12).

The exceptional lipid organization can be ascribed to the unique composition of SC lipids which comprise mostly free fatty acids (FFA), cholesterol (CHOL), and ceramides. SC ceramides represent a unique, heterogeneous group of at least six ceramides (CER(1–6)) that differ from each other by the head group architecture and by the mean fatty acid chain length. The fatty acid esterified to the amide of the (phyto)sphingosine head group can be either α-hydroxy or nonhydroxy fatty acids (13). The fatty acid chain length varies between 16 C atoms in CER 5 to C30–C34 atoms in CER 1. Furthermore, CER 1, a ceramide assumed to be of importance for proper SC barrier function (14) contains linoleic acid linked to the long chain (C > 30) ω-hydroxy fatty

Abbreviations: SC, stratum corneum; CER, ceramide; FFA, free fatty acids; CHOL, cholesterol; PA, palmitic acid

[1]To whom correspondence should be addressed.

acid. The molecular architecture of the pig ceramides is depicted in **Fig. 1**.

Recently the lipid organization of isolated pig skin ceramides (CER(1–6)), cholesterol (CHOL), and free fatty acids (FFA) has been examined (15, 16). These studies revealed that mixtures of CER and CHOL at confined molar ratios mimic the lipid phase behavior of intact SC very closely. Two lamellar phases were formed with repeat distances of 12.2 and 5.2 nm, respectively. When long-chain FFA were added (the major fractions being C24 and C26), the periodicity of the lamellar phases increased slightly to 13.1 and 5.3 nm, respectively, mimicking the SC lipid phase behavior even more closely. Furthermore, the presence of FFA increased the solubility of CHOL, which might be essential for the barrier function of the skin. In the present investigation we have extended the study of the role the individual ceramides play in lamellar lipid organization. We have especially focused our attention on CER 1, which due to its unusual structure (13) may play a key role in the SC lipid organization. The role of CER 1 has been recently studied (17) with a 2:2:1 molar mixture prepared from CHOL and palmitic acid (PA) mixed with either CER(2–5) or CER(1–5). These experiments revealed that under these conditions CER 1 promoted the formation of the long periodicity phase. Although this study was carried out carefully, the lipid mixture used was not representative for the pig SC lipid composition, as CER 6, which is present in pig skin in significant amounts (6% w/w) was not included and the only FFA included

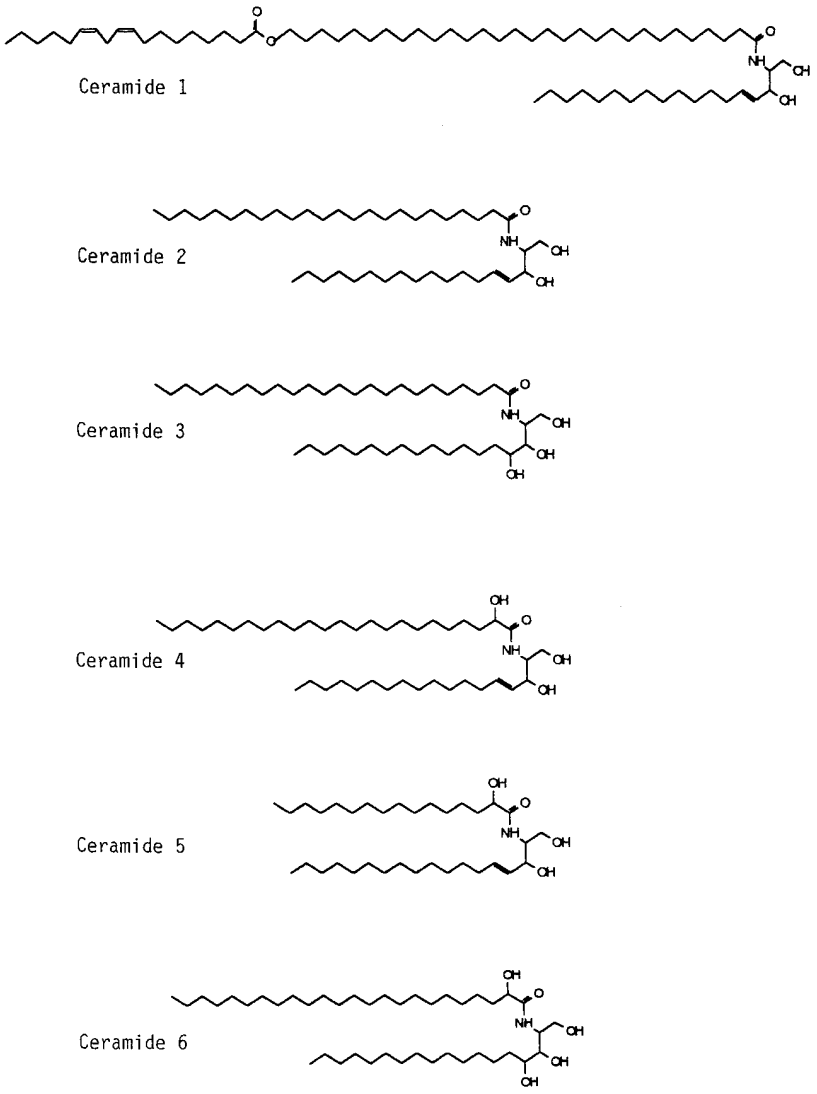

Fig. 1. The molecular structures of pig ceramides published by Wertz and Downing (13). Ceramide 6a is not included in this scheme as it has been reported in a recent paper (29) that CER 6 is most probably an oxidation product produced from CER 1 during fractionation.

was free PA, although the content of free PA in SC is low (18). Furthermore, the pH was not controlled and water was used for the hydration of the lipid mixtures. As we have recently observed that both pH and CER 6 affect the phase behavior of SC lipid mixtures (J. A. Bouwstra, F. E. R. Dubbelaar, G. S. Gooris, W. Weerheim, and M. Ponec, unpublished results) and, furthermore, short-chain fatty acids when mixed with CER(1–6) and CHOL phase separate (15), we decided to study the role of CER 1 in the formation of the long periodicity phase in CHOL/CER(1–6)/FFA mixtures in more detail. For this purpose CER(2–6) mixtures were prepared. These mixtures were then mixed with CHOL and long-chain FFA (the major chain lengths being C22 and C24) and their phase behavior was studied by X-ray diffraction over a wide range of molar ratios at a pH of 5, being the pH of the surface of the skin (19). The phase behaviors of these mixtures were compared with those prepared from CHOL/CER(1–6)/FFA, thus including CER 1. In addition, electron density calculations were performed and a molecular organization for the two lamellar phases was proposed. In this model the short periodicity phase is composed of only one bilayer, while the long periodicity phase consists of two broad and one narrow, low electron density regions.

EXPERIMENTAL

Isolation of stratum corneum from pig skin

Fresh pig skin was obtained from a slaughter house and SC was isolated from the skin as described before (15).

Extraction, separation, and identification of lipids from stratum corneum

Epidermal lipids were extracted using the method of Bligh and Dyer (20). The extracted lipids were applied on a silica gel 60 (Merck) column with a diameter of 2 cm and a length of 33 cm. The various lipid classes were eluted sequentially using various solvent mixtures as published recently (15). The lipid composition of collected fractions was established by one-dimensional high performance thin-layer chromatography, as described before (21). For quantification, authentic standards (Sigma) were run in parallel. The quantification was performed after charring using a photodensitometer with automatic peak integration (Desaga, Germany). Isolated fractions were mixed to achieve mixtures of CER(2–6) or mixtures of CER(1–6).

Preparation of lipid mixtures

The ceramides and CHOL were mixed in various molar ratios, using a mean ceramide molar weight of 700 and 671 for CER(1–6) and CER(2–6), respectively. For calculation of the mean ceramide molecular weight, the data on the ceramide composition and alkyl chain length distributions (13) were used. A pH 5 was chosen, as that is the pH of the skin surface (19). Mixtures were prepared from either CHOL and CER(1–6) or CHOL, CER(2–6) and FFA as described before (15). Briefly, the mixture was dissolved in chloroform–methanol 2:1 at the desired composition and applied on mica at a very low rate (4.2 μl/min) under a stream of nitrogen. The applied lipid mixture was then heated to approximately 100°C and kept at this temperature for a few minutes and cooled down to 80°C, after which the mixture was covered with 1–2 ml 10 mM acetate buffer, pH 5.0, and kept under nitrogen. Subsequently, the samples were quenched using dry ice. Then the samples were placed in a small Teflon sample holder, after which at least 10 freeze-thawing cycles were carried out between −20°C and room temperature. Until use the samples were stored at −20°C. For the FFA mixture we chose long-chain free fatty acids in a molar ratio according to Wertz and Downing (18). The following fatty acids were included in the lipid mixtures: C16:0, C18:0, C22:0, C24:0 and C26:0 in a molar ratio of 1.3:3.2:41.7:36.8:6.7, respectively.

X-ray diffraction measurements

All measurements were carried out at the Synchrotron Radiation Source at Daresbury Laboratory using station 8.2. This station has been built as a part of a NWO/SERC agreement. The samples were put in a specially designed sample holder with two mica windows. A detailed description of the equipment has been given elsewhere (10). The experimental conditions were similar as described before (15). No orientation of the lipid layers to the primary beam was achieved. This is caused by the crystallinity and the low water content in the lipid samples. The scattered intensities were measured as a function of θ, the scattering angle. Calibration of the detector was carried out with rat tail and cholesterol. From the scattering angle the scattering vector (Q) was calculated $Q = 4\pi(\sin\theta)/\lambda$, in which λ is the wavelength being 0.154 nm at the sample position. Simultaneously with the small angle X-ray diffraction experiments, wide angle X-ray diffraction measurements were carried out using an INEL detector. The measurements were carried out during a period of 10 min. The distance between the sample and INEL detector was set to approximately 0.25 m. The INEL detector was calibrated with cholesterol and Si. The diffraction curves were plotted as a function of Q.

For calculations of the electron density profiles of the long and short periodicity phase, the relative heights of the peaks in the diffraction patterns of the equimolar

CHOL:CER(1–6) mixture and the mixture prepared from CHOL:CER(2–6) in a molar ratio of 0.4 were determined. Smearing of the diffraction pattern by the beam size or the resolution of the detector is negligible, as *i*) the sample–detector distance (SAXD) is 1.4 m, *ii*) the beam cross section is 0.5 × 3 mm^2, and *iii*) the spatial resolution of the detector is 0.4 mm.

RESULTS

Ceramide isolation and preparation of lipid mixtures

Fractions containing CER (1–6) were isolated by column chromatography from extracts of porcine stratum corneum lipids. Isolated ceramide fractions were mixed to prepare mixtures of CER(2–6) in the same proportions as present in pig SC. The CER(2–6) or CER(1–6) mixtures were subsequently mixed with CHOL at varying molar ratios or in equimolar ratios with both CHOL and FFA. The composition of CER(2–6) in weight percentages is 43.2, 25.8, 5.3, 19.3, and 6.3% for CER 2, CER 3, CER 4, CER 5, and CER 6, respectively. The composition of the CER(1–6) has been published recently (15, 22).

Phase behavior of lipid mixtures

Lamellar phases. The X-ray diffraction curves of CHOL/CER(2–6) mixtures in molar ratios of 0.2, 0.4, and 1 are presented in **Fig. 2a and b**. The spacings are summarized in **Table 1**. The diffraction curve of the 0.2 molar mixture revealed one strong 5.25 nm peak (Q = 1.20 nm^{-1}) and two weak reflections at 2.62 nm (Q = 2.40 nm^{-1}) and 1.77 nm (Q = 3.55 nm^{-1}) based on a 5.25 nm lamellar phase. In addition, two weak shoulders were observed at approximately 6 nm (Q = 1.05 nm^{-1}) and 4.4 nm (Q = 1.43 nm^{-1}), respectively, which might be based on the 12.2 nm lamellar phase (15). Increasing the CHOL content to a molar ratio of 0.4 revealed a similar diffraction pattern. The strong and weak peaks shifted to 5.21 nm (Q = 1.21 nm^{-1}), 2.61 nm (Q = 2.41 nm^{-1}) and 1.72 nm (Q = 3.65 nm^{-1}), respectively, indicating a slight shift in the periodicity to 5.21 nm. In addition, two weak diffraction peaks appeared at 3.37 and 1.69 nm, respectively, based on crystalline CHOL. Increasing the CHOL content further to a molar ratio of 1 again shifted the main peak to a slightly shorter spacing of 5.16 (1.22 nm^{-1}) nm. In addition, two shoulders observed at lower CHOL content turned into two weak peaks at 6.4 (0.98 nm^{-1}) and 4.4 (1.43 nm^{-1}) nm and the intensity of the reflections based on crystalline cholesterol increased compared to those observed at a molar ratio of 0.4.

Mixtures prepared from CHOL, CER(2–6), and long-chain FFA revealed a similar phase behavior compared to the equimolar mixtures of CHOL and CER(2–6), see Figure 2b. A strong peak at 5.4 nm was observed with two weak shoulders at 6.5 and 4.6 nm on both sides of this peak. Furthermore, peaks based on crystalline CHOL were smaller than observed in the diffraction curve of the equimolar mixture of CHOL and CER(1–6).

In a recent study (15) the phase behavior of mixtures prepared from CHOL/CER(1–6) was investigated. From the intensity of the 3.35 nm diffraction peak based on CHOL it was concluded that the amount of CHOL that phase separated increased with increasing relative amount of CHOL. In this study the solubility of CHOL in lipid mixtures was studied in more detail. At a CHOL/CER(1–6) molar ratio of 0.2 and 0.3, no diffraction peak at 3.35 nm spacing was detected, indicating that no CHOL phase separation occurred. At a molar ratio of 0.4, a small diffraction peak at 3.35 nm spacing is present suggestive of CHOL phase separation. From these observations it was concluded that CHOL in CHOL/CER(1–6) mixture starts to phase separate between a molar ratio of 0.3 and 0.4. Interestingly, between a molar ratio of 0.1 and 0.4, the short periodicity phase decreased in periodicity from approximately 6.7 to 5.2 nm. Further increase of the CHOL content did not result in a further decrease in the periodicity of this phase. It seems that intercalation of CHOL results in a reduction of the bilayer thickness of the short periodicity phase. At a CHOL/CER(1–6) molar ratio of 0.3, the 12.2 nm phase was already formed and did not change in repeat distance upon further increase of the CHOL content.

Lateral packing. The wide angle X-ray diffraction curves of mixtures prepared from CER(2–6) and CHOL at a molar ratio of 0.2, 0.4, and 1 are plotted in Fig. 2c. In these curves, a peak was observed at a spacing of approximately 0.412 nm, indicative of a hexagonal lateral packing. The intensity of this reflection decreased with increasing CHOL content suggesting that a fluidization occurs.

The diffraction pattern of mixtures prepared from CHOL, CER(2–6), and long-chain FFA revealed one strong peak at 0.410 nm and a broader peak at 0.38 nm spacing. The presence of the 0.38 nm peak indicates that at least some lipids transformed from hexagonal to orthorhombic lateral packing.

Model calculations

To propose a model for lipid organization within the short and long repeat units, the electron density distribution was calculated using diffraction curves obtained with either CHOL/CER(2–6) or CHOL/CER(1–6) mix-

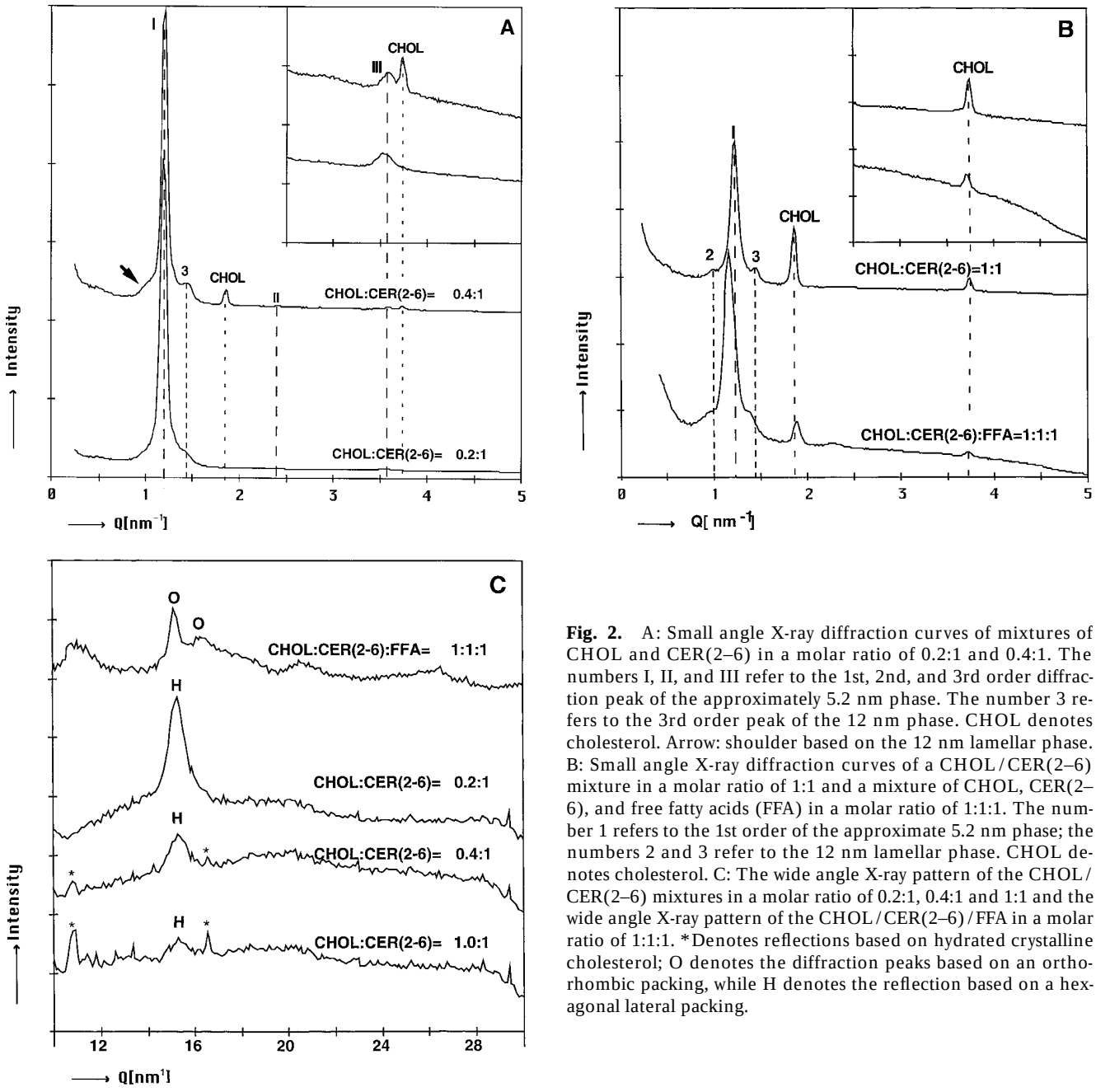

Fig. 2. A: Small angle X-ray diffraction curves of mixtures of CHOL and CER(2–6) in a molar ratio of 0.2:1 and 0.4:1. The numbers I, II, and III refer to the 1st, 2nd, and 3rd order diffraction peak of the approximately 5.2 nm phase. The number 3 refers to the 3rd order peak of the 12 nm phase. CHOL denotes cholesterol. Arrow: shoulder based on the 12 nm lamellar phase. B: Small angle X-ray diffraction curves of a CHOL/CER(2–6) mixture in a molar ratio of 1:1 and a mixture of CHOL, CER(2–6), and free fatty acids (FFA) in a molar ratio of 1:1:1. The number 1 refers to the 1st order of the approximate 5.2 nm phase; the numbers 2 and 3 refer to the 12 nm lamellar phase. CHOL denotes cholesterol. C: The wide angle X-ray pattern of the CHOL/CER(2–6) mixtures in a molar ratio of 0.2:1, 0.4:1 and 1:1 and the wide angle X-ray pattern of the CHOL/CER(2–6)/FFA in a molar ratio of 1:1:1. *Denotes reflections based on hydrated crystalline cholesterol; O denotes the diffraction peaks based on an orthorhombic packing, while H denotes the reflection based on a hexagonal lateral packing.

tures. The background scattering at the positions of the peaks was determined by interpolation of the base line on both sides of the peaks using a straight line. Diffraction peaks that partly overlapped were deconvoluted by assuming that the diffraction peaks were symmetric. This seems to be appropriate, as no smearing of the diffraction pattern occurred. Because a random orientation of the lipids in the sample has been observed (15), the calculated intensities were divided by Q^2, the so-called Lorenz factor. Furthermore, in the model calculations disorder of the first and second kind were neglected.

Short periodicity phase. The peak heights of the short periodicity phase could be accurately determined with the diffraction curve of the CHOL/CER(2–6) mixture in a molar ratio of 0.4, because in this curve the diffraction peaks corresponding to the 12.2 nm phase were weak. In the calculations, the electron density profiles of the head group regions were approximated by a gaussian electron density distribution. To reduce the

TABLE 1. Periodicity (d) of the various phases and the positions of the corresponding reflections found in mixtures of CHOL, CER(2–6), and FFA

CHOL:CER (2–6):FFA	Periodicity of Phase	Reflections	WAXD	CHOL
	nm	*nm*		
0.2:1:0	≈12–13[a]	≈6(2), ≈4.4(3)	0.415[b]	
	5.25	5.25(1), 2.62(2), 1.77(3)		
0.4:1:0	≈12–13[a]	≈6(2), 4.4(3)	0.415[b]	3.37, 1.69
	5.21	5.21(1), 2.62(2), 1.77(3)		
1:1:0	≈12–13[a]	≈6(2), 4.35(3)	0.41[b]	3.37, 1.69
	5.16	5.16(1)		
1:1:1	≈12–13[a]	6.5(2), 4.6(3)	0.415[b]	3.33, 1.68
	5.4	5.4(1), 2.78(2)		

[a]Due to the inaccuracy in the peak positions, only an approximate periodicity and peak positions can be given.

[b]The intensity of this reflection decreased with increasing CHOL content in the CHOL:CER(2–6) mixtures. Addition of FFA increased the reflection in intensity.

number of variables to two, the electron density of the hydrocarbon regions was kept constant. Based on the difference in fatty acid and sphingosine base chain lengths, the terminal methyl groups of the hydrocarbon chains are not expected to be located in the center of the hydrocarbon regions causing a low electron density region. The intensities of the diffraction peaks were calculated by Fourier transformations of the electron density profiles. In an interactive procedure, in which the position and width at half intensity of the gaussian distribution in the electron density profile were systematically varied in steps of 0.002 and 0.01 nm, respectively, the difference between the calculated and experimental peak heights of the diffraction curves was minimized. The experimental intensities of four diffraction peaks were available for the calculations.

Due to the loss of phase information in calculating the intensities from an electron density profile, known as the phase-problem (23), no unique electron density profile could be selected. However, all the selected electron density profiles indicate that the short periodicity phase consists of one bilayer. The electron density profiles differed only slightly in the positions of the head groups. In the various calculated electron density profiles, the distance between the two head group regions in one unit varied between 4.60 and 4.99 nm. An example of the electron density profiles is plotted in **Fig. 3**. The corresponding calculated and experimental intensities are given in **Table 2**.

Long periodicity phase. The electron density calculations of the long periodicity phase were carried out using the diffraction curve of the equimolar mixture of CHOL/CER(1–6). In the model calculations of the electron density profiles of the 12.2 nm lamellar phase, the width and the position of the gaussian distributions were varied systematically. The intensity of the various diffraction peaks was calculated by Fourier transformation of the electron density distributions. The number of independent variables was 4; the number of diffraction peaks was 7. In selecting the optimal electron density profile of the 12.2 nm phase, the difference in

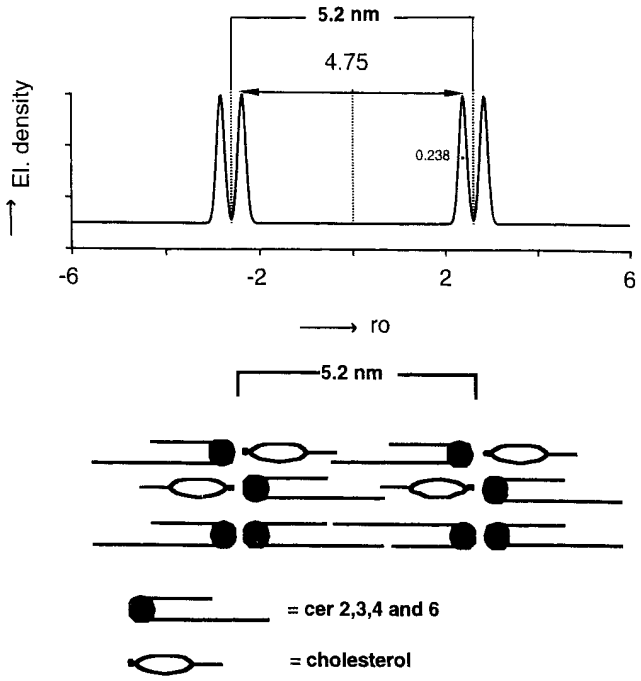

Fig. 3. The calculated electron density of the 5.2 nm lamellar phase plotted as a function of the distance (ro) perpendicular to the basal plane. The head group regions are presented by a gaussian electron density distribution, the width at half maximum being 0.24 nm. The distance between the head group regions is 4.76 nm. However, due to the loss of phase information this distance could not be determined very accurately (see text). Below the electron density profile, the proposed molecular arrangement in this phase, in which only CER(2–6) and CHOL are included, is drawn. The bilayer is formed by two opposite interdigitating ceramides or an interdigitating CHOL and ceramide.

TABLE 2. Experimental and calculated intensities of the 12.2 nm and 5.2 nm phases

Order of Peak	12.2 nm Phase		5.2 nm Phase	
	Experimental Intensity	Calculated Intensity	Experimental Intensity	Calculated Intensity
1	0.78[a]	0.77[a]	557[a]	557[a]
2	1	1	1	1
3	0.54	0.54	3.4	3.5
4	<0.01[b]	0.025	0.20	0.17
5	<0.05	0.045		
6	0.0125	0.011		
7	<0.011	0.004		

[a]The intensity values are relative intensities, in which the second order diffraction peak is set equal to 1.

[b]Three peak intensities could not be determined very accurately, as the peak possibly overlaps with another peak from either the 5.3 nm phase or crystalline CHOL. Therefore, in these cases, only a maximum value for the peak intensity could be given.

intensity between the calculated and experimental diffraction peaks of the curve of the equimolar CHOL/CER mixture was minimized in an interactive procedure, in which in the electron density profile the position and width at half intensity of two gaussian distributions were independently systematically varied in steps of 0.002 and 0.01 nm, respectively. Several electron density profiles were found, the corresponding peak intensities of which all fitted to the experimental ones. Therefore, it was decided to introduce some restrictions that were based on observations, such as *i*) the small size of the ceramide head groups limits the width at half maximum of the gaussian electron density distribution to 0.8 nm, *ii*) a water region between the terminal head group regions was considered to be absent as no swelling of the lamellar phases in SC was observed upon increasing the water content (10, 12), *iii*) the fatty acids linked to ceramides show a bimodal chain-length distribution with the prevailing chain lengths around C24–C26 and C16 (13, 22), and *iv*) the C16 and C24 ceramides do not mix but phase separate even in the presence of large amounts of CHOL, as demonstrated in a recent study in which SC lipid phase behavior in mixed Langmuir-Blodgett monolayers was examined (22). It is therefore likely that the ceramides with fatty acid chain length of C16 and C24 do not accommodate within the lipid layers of the long periodicity phase, but form separate layers in one unit cell. Taking these observations into account and assuming a symmetrical electron density distribution in the unit cell, we decided to vary the position of two gaussian electron density distributions between 1 and 1.2 nm symmetrically from the center of the unit cell. These values were based on the C16 fatty acid chain length prevailing in CER 5 (13) and on the length of the linoleic chain linked to the ω-hydroxy fatty acid of CER 1 (13). Furthermore, the localization of the two remaining gaussian electron density distributions of the terminal head group regions of the unit cell was varied between 5.3 and 6.05 nm from the center of the unit cell, as the ceramides containing C24–C26 fatty acids are more abundantly present than the ceramides containing C16 fatty acids and almost no swelling of the SC lamellar phase was observed in the presence of water. With these restrictions, two broad hydrocarbon chain regions were created. The difference between the calculated and observed intensities of the various diffraction peaks was minimized. The resulting electron density distribution is drawn in **Fig. 4,** the corresponding calculated and experimental intensities of the various diffraction peaks are given in Table 2.

DISCUSSION

Phase behavior of skin lipid mixtures

In a recent study in which the phase behavior of mixtures prepared from CHOL and CER(1–6) was examined (15), we found that over a large range of CHOL/CER(1–6) molar ratios, two lamellar phases were present with repeat distances of 5.2 and 12.2 nm, respectively. The addition of long-chain FFA increased the periodicities of these phases to approximately 5.3 and 13.1 nm, respectively. From these studies it was concluded that the lipid mixtures mimic the lipid phase behavior in SC very closely.

In the present study the role of CER 1 on the SC lipid phase behavior was investigated by studying the phase behavior of CHOL/CER(2–6) mixtures. This phase behavior was compared to that of CHOL/CER(1–6) mixtures (15). In the absence of CER 1, the phase behavior of the lipid mixtures changed quite dramatically: at molar ratios between 0.2 and 1 the short periodicity phase at approximately 5.2 nm was prevailing. On the diffraction curves obtained with these CHOL/CER(2–6) mixtures, the peaks (6.4 and 4.3 nm) based on the long periodicity phase were very weak, indicating that only a small fraction of the lipids is organized in the long periodicity phase. The same observations have been made when long-chain FFA were included in the mixture.

Our observations are in agreement with findings of McIntosh, Stewart, and Downing (17) with a mixture lacking CER 6 and containing only PA. This observation was quite surprising as our recent studies revealed that the presence of CER 6 is important for the formation of the long periodicity phase at high CHOL/CER ratios as used by McIntosh, Stewart, and Downing (17).

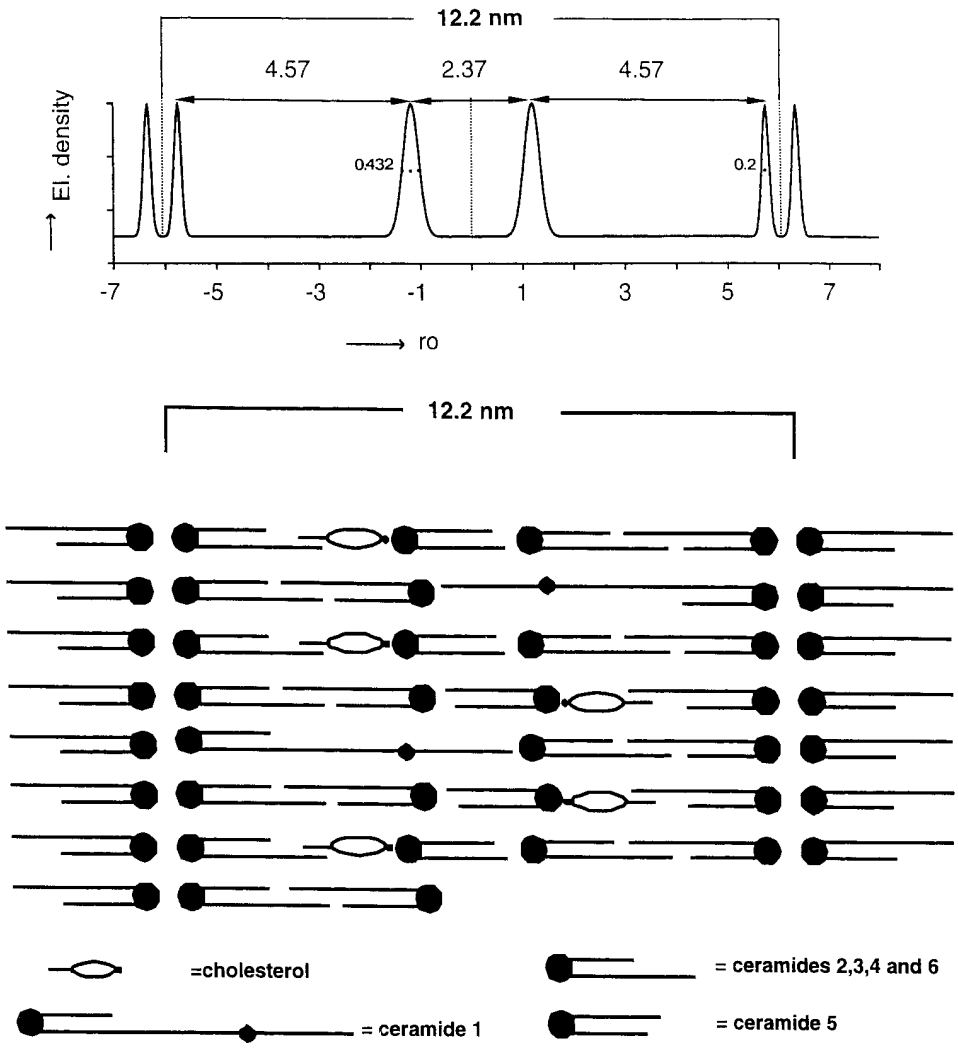

Fig. 4. The calculated electron density profile of the 12.2 nm lamellar phase as a function of the distance (ro) perpendicular to the basal plane. Note that the width at half maximum intensity of the gaussian electron density distribution of the head-groups located on both sides of the narrow low-electron density region is 0.43 nm, which is larger than the width at half maximum intensity of the gaussian electron density distributions located at the boundaries of the unit cell being 0.2 nm in width. Below the electron density profile, the schematic presentation of the proposed molecular arrangement of the 12.2 nm phase, in which the long chain fatty acid ceramides and short chain fatty acid ceramides are localized in separate lipid layers, is drawn. Note the undulation of the head group regions on both sides of the narrow low electron density region in the center of the unit cell. The undulations correspond to the broader gaussian electron density profile in these regions shown in electron density profile. The molecular structures of the various ceramides are drawn in Fig. 1.

In addition, we found that the pH affects the lipid organization (J. A. Bouwstra, F. E. R. Dubbelaar, G. S. Gooris, W. Weerheim, and M. Ponec, unpublished results). Namely, an increase in pH promotes the formation of the long periodicity phase. Furthermore, in the presence of the short-chain FA, phase separation occurs. The finding of the formation of the long periodicity phase with CHOL/CER(1–5)/PA mixtures prepared at a molar ratio of 2:2:1 and hydrated with water (17) indicates that a compensation of the 'negative effects' of the above-mentioned factors may occur.

The lateral packing in the mixtures of the CHOL/CER(2–6) is mainly hexagonal similar to that seen in CHOL/CER(1–6) mixtures. In contrast to observations made with CHOL/CER(1–6) mixtures, in the diffraction pattern of the CHOL/CER(2–6) mixtures the 0.415 nm reflection based on the hexagonal lateral packing decreased in intensity with increasing CHOL content. This strongly indicates a decrease in the ordering of the lateral packing and a phase change from a hexagonal to a liquid lateral packing. The finding that the presence of CER 1 favors the formation of the long-periodicity phase and an ordered lipid lamellar packing clearly indicates the important role CER 1 plays in

the formation of the long periodicity phase and the hexagonal lateral packing.

Molecular arrangement in the lamellar phases

Long periodicity phase. We propose that SC lipid lamellae consist of three lipid layers, in which the ceramides are either partly interdigitating (the broad low-electron density layers) or fully interdigitating (the narrow low-electron density layers), see Fig. 4. The two broad low-electron density regions are formed by ceramides, with the long-chain fatty acids (predominantly C24 to C26) linked to the (phyto)sphingosine backbone, and CHOL, while the narrow low-electron density region is formed by the short-chain ceramides (predominantly C16). This molecular model is based on *a*) the calculated electron density profile that consists of one narrow and two broad low-electron density regions, *b*) the importance of CER 1 for the formation of the long periodicity phase, and *c*) observations from other studies, the most important being *i*) the bimodal fatty acid chain-length distribution of the ceramides (13), *ii*) the phase separation between ceramides with long-chain fatty acids and ceramides with short-chain fatty acids as observed in the monolayer approach (22) and *iii*) the absence of swelling upon increasing the water content in SC (8, 9). In this molecular model, CER 1 plays an important role in the formation of the long periodicity phase as it dictates the broad-narrow-broad sequence in the structural unit. Moreover, the formation of this phase is facilitated by the presence of ceramides with C14–C16 fatty acids. An extended C16 chain is about 1.9 nm, approximating the width of the hydrophobic region in the narrow low electron density region (1.8 nm). The C16 chain length is predominantly present in CER 5 (13) and therefore CER 5 is expected to be located in the narrow low electron density region. In the absence of CER 5 the function of this ceramide can most probably be partly taken over by CHOL. Recently we have shown that CHOL/CER(1,2) mixtures form the long periodicity phase only at high CHOL/CER(1,2) molar ratios ($>$0.6) (24), which indirectly substantiates the possible replacement of CER 5 by CHOL.

The proposed model strongly suggests that if the short-chain ceramide is present for the formation of the narrow electron density region, the solubility of CHOL in the long periodicity phase in the CHOL/CER (1–6) mixture reaches saturation at a molecular ratio of approximately 0.2. The low solubility of CHOL in the long periodicity phase is supported by the finding that the diffraction peaks of the long periodicity phase do not change in position and intensity in CHOL/CER(1–6) mixtures exceeding a molar ratio of 0.3, while the periodicity of the 6 nm phase decreases until a molar ratio of 0.4 is reached. In SC the solubility of CHOL is much higher due to the presence of FFA (15) and other lipids such as cholesterol sulfate (recent observations from our laboratory).

The CHOL molecules with their short hydrocarbon tail and the long chain ceramides partly interdigitate in the broad low-electron density regions similarly as in the short periodicity phase, see below (Fig. 3). In order to find out whether a CHOL and a ceramide with a long chain fatty acid can be integrated in one lipid layer, molecular modelling calculations were carried out. For this purpose we used the crystal structure of N-tetracosanoyl-phytosphingosine published by Dahlen and Pascher (25). The two alkyl chains in this structure are present as a V-shaped element. A conformation in which the two alkyl chains were arranged in a more parallel fashion, however, was energetically equally feasible. We further analyzed this conformation (referred to as C24 CER), as it approaches the bilayer organization much better. Molecular modelling calculations revealed a difference in length of approximately 0.8 nm between the longest axis of two opposite interdigitating C24 CERs (hydrophobic core approximately 4.8 nm) and the longest axis of an interdigitating C24 CER and CHOL (hydrophobic core approximately 4 nm), demonstrating that intercalation of the CHOL in the lipid layers creates some space in these layers. CHOL might therefore induce a phase change to a less tight lateral packing. This is in agreement with our recent observations, in which we found that while a ceramide mixture forms crystalline phases (15), the addition of CHOL induces a transition from a crystalline to a hexagonal lateral packing. The created space can partly be compensated for by the undulations of ceramide head groups on both sides of the narrow hydrocarbon region in the center of the unit cell, see Fig. 4. This might be one of the reasons why the bilayer stacking of the long periodicity phase is highly ordered, as demonstrated by the high number of diffraction peaks often found in the diffraction curve of this phase. Finally, the undulations of the head group positions would reduce the width of the broad and narrow low electron-density region and increase the width of the two high electron density head-group regions close to the center of the membrane. This hypothesis is supported by the results of the electron density calculations, although the width of the headgroup regions might be somewhat underestimated. A requirement for the proposed molecular arrangement is that the surface areas of cholesterol and ceramides are approximately equal. This has been recently observed in experiments in which the phase behavior of SC lipids was examined using the monolayer approach (22). Studies with Langmuir-Blodgett films revealed that the surface area per molecule of pig ceramides and CHOL are very similar at high surface pres-

sures. High surface pressures are expected to be present in a crystalline or hexagonal phase observed in these CHOL/CER lipid mixtures.

The results of the present study clearly show that in the absence of CER 1 only a small proportion of lipids in CHOL/CER(2–6) mixtures form the long periodicity phase. From these observations it was concluded that CER 1 is required for proper organization of lipophilic regions in this phase, the long C30–C34 ω-hydroxy-chain of CER 1 fits into the broad hydrocarbon regions, while the short linoleic chain fits into the narrow hydrocarbon region (Fig. 4). Interestingly the length of the completely extended ω-hydroxy C30–C34 fatty acid chain is approximately 4.0 nm, similar to the width of the hydrophobic core of the interdigitating CER and CHOL. The presence of CER 1 in the structure creates space that can be filled by long chain fatty acids, which would make the structure more tightly packed (Fig. 4). This is in agreement with recent observations; long chain fatty acids induce a transition from a hexagonal to an orthorhombic lateral packing (see Fig. 2c and paper in preparation).

The calculated electron density profile and the molecular arrangement of the lipids correlates with the broad-narrow-broad pattern observed in the electron micrographs of SC stained and fixed with ruthenium tetraoxide (4, 26). Based entirely on this appearance, a molecular model was proposed by Swarzendruber et al. (4). In both models the central role of CER 1 is obvious: it is the ceramide that links the narrow and broad low-electron dense regions. However, their model differs in many aspects from our model, as summarized in **Table 3**. The most important difference is that in our model the ceramides have a tail-to-tail double arrangement in the lipid layers, while the ceramides in their model are arranged in a planar alignment (4). As a consequence, their molecular model suggests that the interfacial area of the ceramides in planar alignment and CHOL should be approximately equal, which is not in agreement with published data. Dahlen and Pascher (27) reported that the interfacial area of the ceramides in a planar alignment is approximately 0.25 nm^2. This is different from the interfacial area of CHOL, which is approximately 0.37 nm^2 (28). By contrast, the interfacial area per ceramide molecule having a tail-to-tail double arrangement is predicted to be approximately 0.40 nm^2 (27). Therefore, our model, in which the CHOL and ceramides have an equal interfacial area, is in agreement with these data.

Short periodicity phase. As could be concluded from the electron density calculations, the short periodicity phase consists of only one bilayer. As no swelling in the SC lamellar phases was seen upon increasing the water content (8, 9), most probably the terminal head groups in adjacent unit cells are located very closely to each other. Despite the difference in length between two opposite interdigitating CERs and a CER and CHOL, CHOL most probably is intercalated in the bilayer at a position similar to the ceramides. This conclusion is based on the observation that increasing CHOL content in the CHOL/CER(1–6) mixtures from a molar ratio of 0.1 to 0.4 caused a decrease in the periodicity of the short periodicity phase from 6.7 to 5.2 nm. It is likely that the extent of interdigitation of a CER and CHOL is reduced by decreasing the CHOL/CER molar ratio. This decrease in the extent of interdigitation will reduce the difference in length of two opposite interdigitating CER and of the CER + CHOL and most probably increases the hydrophobic interaction between the cholesterol molecule and the surrounding ceramides. Finally, in the short periodicity, the solubility of CHOL is expected to be large reaching a CHOL/CER(1–6) molecular ratio of at least 0.5 and possibly even higher.

In conclusion, the present study reveals that CER 1 is of great importance for the formation of the lateral lipid packing as well as the long range lamellar ordering in SC. A decrease in the CER 1 content in stratum corneum will most probably result in a decrease in the proportion of lipids organized in the long periodicity phase in SC as observed in the present study with the lipid mixtures and in recent studies performed with

TABLE 3. Summary of the differences in the molecular organization of the long periodicity phase presented in this paper and proposed previously (4)

SC Lipid Arrangement Items	Model Presented in This Paper	Previously Proposed Model (4)
Ceramide arrangement	tail to tail double	planar
Role of CER 5	central	none
Mixtures of CER with long- and short-chain fatty acids	phase separation[a]	no phase separation
Role of lipids covalently bound to the cornified envelope	none[b]	important

[a]Phase separation between long- and short-chain CER has been found in the monolayer approach (22).
[b]Lamellar phase is formed in lipid mixtures in their absence (15).

human SC (V. Schreiner, S. Pfeifer, E. Proksch, and J. A. Bouwstra, unpublished results). In addition, the long range ordering exhibits a very exceptional molecular arrangement in which long-chain and short-chain ceramides are arranged in separate lipid layers, forming a broad-narrow-broad sequence in the 12 nm lamellar phase. The molecular organization for the long and short periodicity phases clearly shows that for the formation of the two lamellar phases in the stratum corneum not only the head group architecture but also the fatty acid chain length in individual ceramides and the differences in the chain length between the fatty acid and the (phyto)sphingosine base are very important. In addition, the results presented in this paper and other recent reports (15, 17) clearly demonstrate that for the formation of the long periodicity phase no proteins are required, as was suggested in earlier X-ray diffraction studies on intact SC (8, 9, 11).

Manuscript received 24 February 1997, in revised form 1 July 1997, and in re-revised form 4 September 1997.

REFERENCES

1. Elias, P. M. 1983. Epidermal lipids, barrier function, and desquamation. *J. Invest. Dermatol.* **80:** 44s–49s.
2. Boddé, H. E., M. A. M. Kruithof, J. Brussee, and H. K. Koerten. 1989. Visualization of normal and enhanced $HgCl_2$ transport through human skin in vitro. *Int. J. Pharm.* **253:** 13–24.
3. Breathnach, A. S., T. Goodman, C. Stolinky, and M. Gross. 1973. Freeze-fracture replication of cells of stratum corneum of human epidermis. *J. Anat.* **114:** 65–81.
4. Swarzendruber, D. C., P. W. Wertz, D. J. Kitko, K. C. Madison, and D. T. Downing. 1989. Molecular models of intercellular lipid lamellae in mammalian stratum corneum. *J. Invest. Dermatol.* **92:** 251–257.
5. Holman, B. P., F. Spies, and H. E. Boddé. 1990. An optimized freeze-fracture replication procedure for human skin. *J. Invest. Dermatol.* **94:** 332–335.
6. Mak, V. H. M., R. O. Potts, and R. H. Guy. 1991. Does hydration affect intercellular lipid organization in the stratum corneum? *Pharm. Res.* **8:** 1064–1065.
7. Gay, L. C., R. H. Guy, G. M. Golden, V. M. W. Mak, and M. L. Francoeur. 1994. Characterization of low-temperature lipid transitions in human stratum corneum. *J. Invest. Dermatol.* **103:** 233–239.
8. White, S. H., D. Mirejovsky, and G. I. King. 1988. Structure of lamellar lipid domains and corneocyte envelopes of murine stratum corneum. An X-ray diffraction study. *Biochemistry.* **27:** 3725–3732.
9. Bouwstra, J. A., G. S. Gooris, J. A. van der Spek, S. Lavrijsen, and W. Bras. 1994. The lipid and protein structure of mouse stratum corneum: a wide and small angle diffraction study. *Biochim. Biophys. Acta.* **1212:** 183–192.
10. Bouwstra, J. A., G. S. Gooris, W. Bras, and D. T. Downing. 1995. Lipid organization in pig stratum corneum. *J. Lipid. Res.* **36:** 685–695.
11. Bouwstra, J. A., G. S. Gooris, M. A. Salomons-de Vries, J. A. van der Spek, and W. Bras. 1992. Structure of human stratum corneum as function of temperature and hydration. A wide angle X-ray diffraction study. *Int. J. Pharm.* **84:** 205–216.
12. Bouwstra, J. A., G. S. Gooris, J. A. van der Spek, and W. Bras. 1991. Structural investigations of human stratum corneum by small angle x-ray scattering. *J. Invest. Dermatol.* **97:** 1004–1012.
13. Wertz, P. W., and D. T. Downing. 1983. Acylglucosylceramides of pig epidermis: structure determination. *J. Lipid. Res.* **24:** 753–758.
14. Bowser, P. A., D. H. Nugteren, R. J. White, U. M. T. Houtsmuller, and C. Pottrey. 1985. Identification, isolation and characterization of epidermal lipids containing linoleic acid. *Biochim. Biophys. Acta.* **834:** 419–428.
15. Bouwstra, J. A., G. S. Gooris, K. Cheng, A. Weerheim, W. Bras, and M. Ponec. 1996. Phase behavior of isolated skin lipids. *J. Lipid. Res.* **37:** 999–1011.
16. Bouwstra, J. A., G. S. Gooris, A. Weerheim, K. Cheng, and M. Ponec. 1995. Isolated stratum corneum lipids as model membrane for skin barrier. *Proc. Int. Symp. Controlled Release of Bioactive Material.* **22:** 11–12.
17. McIntosh, T. J., M. E. Stewart, and D. T. Downing. 1996. X-ray diffraction analysis of isolated skin lipids: reconstitution of intercellular lipid domains. *Biochemistry.* **35:** 3649–3653.
18. Wertz, P. W., and D. T. Downing. 1991. Epidermal lipids. *In* Physiology, Biochemistry, and Molecular Biology of the Skin. Volume I. L. A. Goldsmith, editor. Oxford University Press, Oxford. 205–236.
19. Aly, R., C. Shirley, B. Cumico, and H. I. Maibach. 1978. Effect of prolonged occlusion on the microbial flora, pH, carbon dioxide and transepidermal water loss on human skin. *J. Invest. Dermatol.* **71:** 378–381.
20. Bligh, E. G., and W. J. Dyer. 1959. A rapid method of total lipid extraction and purification. *Can. J. Biochem. Physiol.* **37:** 911–917.
21. Ponec, M., A. Weerheim, J. Kempenaar, A. M. Mommaas, and D. H. Nugteren. 1988. Lipid composition of cultured human keratinocytes in relation to their differentiation. *J. Lipid. Res.* **29:** 949–962.
22. ten Grotenhuis, E., R. A. Demel, M. Ponec, D. R. de Boer, J. C. van Miltenburg, and J. A. Bouwstra. 1996. Phase behavior of stratum corneum lipids in mixed Langmuir-Blodgett monolayers. *Biophys. J.* **71:** 1389–1399.
23. Levine, Y. K. 1973. X-ray diffraction studies of membranes. *Prog. Surf. Membr. Sci.* **3:** 279–352.
24. Bouwstra, J. A., K. Cheng, G. S. Gooris, A. Weerheim, and M. Ponec. 1996. The role of ceramides 1 and 2 in the stratum corneum lipid organisation. *Biochim. Biophys. Acta.* **1300:** 177–186.
25. Dahlen, B., and I. Pascher. 1972. Molecular arrangements in sphingolipids. Crystal structure of N-tetracosanoyl phytosphingosine. *Acta Crystallogr. Sect. B.* **28:** 2396–2404.
26. Downing, D. T. 1991. Lipid and protein structures in the permeability barrier of mammalian epidermis. *J. Lipid. Res.* **33:** 301–313.
27. Dahlen, B., and I. Pascher. 1979. Molecular arrangements in sphingolipids. Thermotropic phase behaviour of tetracosanoylphytospingosine. *Chem. Phys. Lipids.* **24:** 119–133.
28. Small, D. 1986. The Physical Chemistry of Lipids. Plenum Press, New York. 407.
29. Wertz, P. W. 1996. The nature of the epidermal barrier: biochemical aspects. *Adv. Drug Delivery Rev.* **18:** 283–294.